Photodetachment of He^- near the 1*s* threshold: Absolute cross-section measurements and postcollision interactions

R. C. Bilodeau,[1,2] J. D. Bozek,[2] G. D. Ackerman,[2] A. Aguilar,[2,3,*] and N. Berrah[1]
[1]*Physics Department, Western Michigan University, Kalamazoo, Michigan 49008-5151, USA*
[2]*Advanced Light Source, Lawrence Berkeley National Laboratory, Berkeley, California 94720, USA*
[3]*Department of Physics, University of Nevada, Reno, Nevada 89557-0058, USA*
(Received 31 October 2005; published 6 March 2006)

Inner-shell photodetachment of He^- is studied near the He^- $1s2s2p\ ^4P^o \rightarrow He\ 2s2p\ ^3P^o$ threshold. The spectrum over this region shows significant suppression of He^+ signal production due to postcollision interaction (PCI) effects. The observed shape and absolute cross section are in general agreement with theoretical predictions when corrections for semiclassical PCI effects are included.

DOI: 10.1103/PhysRevA.73.034701 PACS number(s): 32.80.Gc, 32.80.Hd, 32.30.Jc

Photodetachment and excitation of inner-shell electrons in negative ions is a new field, with initial experiments published in 2001 studying Li^- [1] and Na^- [2]. Negative ions are typically bound in the short-ranged induced-dipole potential ($\propto r^{-4}$), which gives rise to significant qualitative differences between structure and spectra of negative ions and those of neutral and positive atomic systems. He^- is the smallest prototype negative ion, and offers an important model system that is accessible to advanced theoretical treatment. As such, core photodetachment and excitation of He^- has been the subject of extensive theoretical study (see [3–8] and references therein) and was first studied experimentally only about 3 years ago by Berrah *et al.* [9]. Since then, detailed investigations of He^- core-excited resonances, including line position, widths, and absolute cross sections, were conducted [10] and, very recently, investigations of the photodetachment threshold laws in He^- and S^- were also performed [11].

The work by Berrah *et al.* [9] first suggested that the cross section near the He^- $1s2s2p\ ^4P^o \rightarrow He\ 2s2p\ ^3P^o$ threshold may be considerably smaller than expected. However, direct measurements of the absolute cross section were not available, and the absolute scale of the experiment was established by scaling the data at 42 eV to the theoretical cross section calculated by Zhou *et al.* [5]. Later, recapture of the photoelectron (i.e., the "threshold electron") through postcollision interaction (PCI) effects was considered [7] and found to yield better agreement with the apparent lower cross section just above the threshold.

We investigate here the cross section over a region covering 1.3 eV near to and above the He $2s2p\ ^3P^o$ threshold and compare it to calculations. A greatly improved agreement with the shape of the cross section is found when PCI effects are included, underlining the importance of this process in near-threshold photodetachment. Measured absolute cross sections, previously unavailable in this region, are consistent with recent theory.

The experiments were performed at the Advanced Light Source (ALS) Ion-Photon Beamline [12]. A beam of negative atomic He ions was produced using a National Electrostatics Corporation (NEC) rf Rb-vapor charge-exchange ion source [13]. A beam of He^+ was extracted and accelerated to 2.99 keV from an rf source through a Rb vapor cell, where He^- was produced in the metastable $1s2s2p\ ^4P^o$ state [14] by double charge exchange with the Rb atoms. The ions are then further accelerated to 9.96 keV, separated from residual neutral He atoms and contaminant ions with a sector magnet, and directed to 90° electrostatic spherical-sector deflectors that merge the ion beam with a counterpropagating photon beam from the ALS beamline 10.0.1. After a drift of about 1.5 m, a magnetic demerging field separated the He^- beam from the photon beam and directed it into a Faraday cup where typical ion currents of 50–100 nA were observed.

The photon-ion interaction in the merged region can lead to two-electron loss from photodetachment followed by Auger decay (see Fig. 1 for a level diagram). The resulting He^+ ions (the signal) were deflected in a direction opposite to the He^- beam in the demerging magnetic field and counted by a multichannel plate based detection and counting system. Typical rates of ≈50 kHz were observed from collisional

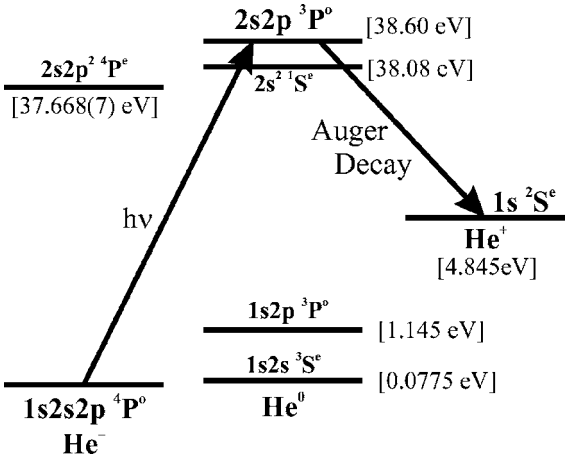

FIG. 1. Partial energy level diagram for He^-, He, and He^+ (not to scale). Energies are relative to the He^- $1s2s2p\ ^4P^o$ metastable ground state. The He $1s^2\ ^1S^0$ ground state (not shown) is at −19.7388 eV on this scale. Arrows indicate the photodetachment and Auger decay steps.

*Present address: Jet Propulsion Laboratory, California Institute of Technology, Pasadena, CA 91109.

stripping with residual background gas ($\approx 5 \times 10^{-10}$ Torr). This background signal was subtracted by chopping the photon beam at 6 Hz.

For absolute cross-sections measurements, the interaction volume must be well defined. This was achieved by the application of +0.506(10) kV to a 29.4-cm-long cylindrical chamber in the merged-beam section [uncertainties are quoted to 1 standard deviation (SD) throughout]. The signal ions produced in this region, therefore, had their kinetic energy increased by 1.012 kV, and could be selected with kinetic-energy analyzing electrostatic spherical-sector deflectors (SSD) positioned just before the positive-ion detector. The interaction region is thus well defined in space, with an effective length of 28.95 cm for the present experimental parameters, as determined from electrostatic simulations using SIMION 7.00 and the ion kinetic energy acceptance of the SSD. The energy-tagging effectiveness was verified by observing that the signal rate reduced to <1 Hz with 0 V applied to the chamber, indicating that $<0.02\%$ of the measured signal originated from ions outside of the interaction region.

The photon energy scale was calibrated against accurately known (±1 to 5 meV) absorption lines of atomic Ne and Ar [15] between 26.5 and 48 eV. The monochromator scanning appeared to be linear over this region and the uncertainty in the calibrated lab-frame photon energy is estimated to be 7 meV. The ion velocities are sufficient to produce a significant ion-frame Doppler shift. The interaction region beam energy of 10.46(11) keV was determined by direct measurement of the interaction region bias potential and the extraction and acceleration potentials of the ion source. For ions counterpropagating with the photons, an ion-frame Doppler increase in the photon energy of 91–94 meV is obtained for photon energies used in this experiment. Possible angular detuning of the ion beam relative to the photon beam is limited by the geometry of the interaction region to be $<5^\circ$, producing an error in the Doppler shift of <0.3 meV in the present experiment. The total Doppler correction uncertainty is estimated to be 0.6 meV over this energy region.

The collected spectra were obtained by scanning the monochromator repeatedly over the photon energy region and summing the individual scans. This serves to minimize the risk of distortion from slight changes of the ion-photon beam overlap and other experimental parameters over time. In addition, all scans are scaled to the continuously monitored photon flux and negative ion current. No significant variation was observed between individual scans.

Figure 2 shows the measured He^+ production near to and just above the 1*s* photodetachment threshold. For a purely sequential photodetachment plus Auger decay process, the He^+ production rate would simply follow the He^- 1*s* photodetachment cross section. However, due to the short decay lifetime of the He $2s2p\ ^3P^o$ hollow-atom state (width of $\Gamma = 8.14$ meV, i.e., ≈ 40 fs [16]), there is a significant probability for the photoelectron to be recaptured through PCI effects and thus suppress He^+ production. This was suggested as the main source of the discrepancy between the observed [9] and calculated [7] He^- photodetachment cross sections.

The photoelectron escape probability P_{esc} can be modeled within the semiclassical approximation with (in atomic units) [17]

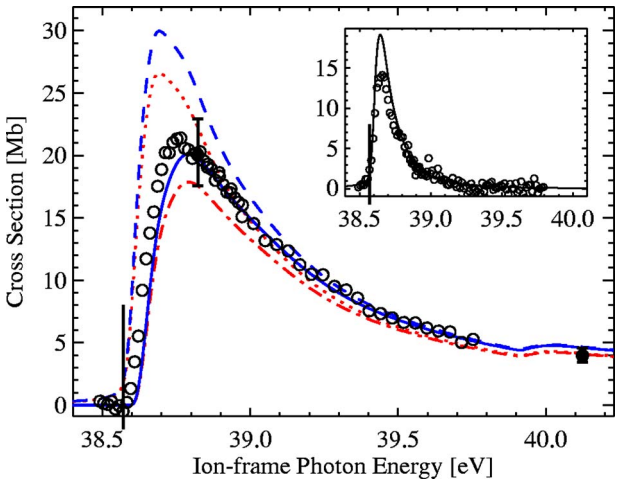

FIG. 2. (Color online) Measured He^+ production (open circles) following photodetachment near the 1*s* threshold, scaled to the measured absolute cross section (filled circles) and with the below-threshold production level (0.37 Mb) subtracted. Curves are theory by Sanz-Vicario *et al.* and PCI correction [7] (dotted and dash-dot, respectively), and scaled by a factor of 1.13 to agree with the data above 39.5 eV (dashed and solid, respectively). The vertical bar at 38.570 eV marks the calculated threshold position. The inset shows the corresponding recaptured portion of the signal, with the curve being the expected level based on the PCI model (i.e., the difference between the dashed and solid curves).

$$P_{esc} = e^{-\Gamma/\sqrt{2\epsilon_e^3}}, \tag{1}$$

where $\epsilon_e = h\nu - \epsilon_t$ is the photoelectron energy and ϵ_t is the photodetachment threshold energy. From the He $1s^2$ energy (−79.003 53 eV [18,19]), the $2s2p\ ^3P^o$ energy (−20.691 20 eV [16,19]), the He $1s2s\ ^3S$ excitation energy (19.819 63 eV [20]), and the He^- $1s2s2p\ ^4P^o$ binding energy to He $1s2s\ ^3S$ (0.077 52 eV [21]), we can obtain an expected $He^-\ 1s2s2p\ ^4P^o \rightarrow He\ 2s2p\ ^3P^o$ threshold energy of 38.5702 eV. P_{esc} is plotted as a function of photon energy in Fig. 3.

The calculated spectra of Sanz-Vicario *et al.* [6] (convoluted with a 30 meV spectral bandwidth) are shown with the dotted curve in Fig. 2. Very similar predictions are obtained with other theoretical approaches [5,8]. The PCI-corrected theoretical He^+ signal (i.e., the product of the total calculated cross section and P_{esc}) is shown by a dot-dashed curve in Fig. 2. We note that the absolute cross-section measurements (filled circles, see below) agree with the PCI-corrected theory to 1 SD. For ease of comparison, the theoretical total (dashed curve) and PCI corrected (solid curve) cross sections are also shown scaled by a factor of 1.13 to agree with the measurements at photon energies above 39.5 eV, where PCI effects are expected to be negligible. The shape of the PCI-corrected curve is in excellent agreement with the data, except very near the threshold. While the deviation near the threshold could be effectively eliminated by shifting the measured spectrum by 15 meV, this is beyond the expected uncertainty of the photon energy calibration (7 meV). As previously noted in Ref. [11], other possibilities include a

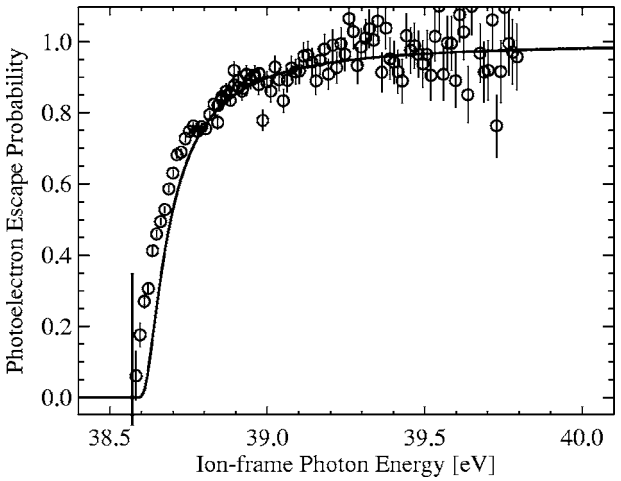

FIG. 3. Photoelectron escape probability based on the semiclassical PCI estimate. The vertical bar marks the calculated threshold position 38.570 eV. Data points are obtained from the ratio of the measured data to the calculated total cross section (dashed curve of Fig. 2).

shift of the calculated $2s2p\ ^3P^o$ energy (used above to obtain the $2s2p\ ^3P^o$ energy), an overestimation of the autoionization width, or possibly a failure of the semiclassical PCI correction at this level of analysis.

The difference between the calculated total photodetachment cross section and the measured He^+ production is shown in the inset of Fig. 2. This signal represents the portion of the total cross section for which PCI effects result in the recapture of the photoelectron and thus the production of neutral He instead of He^+. This signal could in principle be observed as a large increase in He production, however it is not possible to detect neutral products with the current apparatus.

Absolute cross sections were obtained at two photon energies listed in Table I (for completeness, previous absolute cross-section measurements [10], taken at different energies, are also listed). The method employed for the measurements is similar to that used for experiments preformed previously with this apparatus on positive ions [12]. The cross section σ can be obtained from the signal rate R, photon flux Φ (measured by an absolutely calibrated Si x-ray photodiode), and the magnitude of the target ion current I, velocity v, and charge $q=1$, using

TABLE I. Measured absolute cross sections, reported to 1 SD.

Photon energy (eV)	Cross section (Mb)	Reference
37.668(7)	$67(+12/-10)^a$	[10]
38.823(7)	$20(+3/-3)$	Present work
40.128(7)	$4.3(+7/-6)$	Present work
42.969(4)	$41(+7/-6)^a$	[10]
43.160(4)	$3.6(+6/-5)$	[10]
43.536(4)	$5.5(+9/-8)^a$	[10]

[a]These cross sections were obtained on narrow structures, and have been corrected for the spectral bandwidth; see Ref. [10].

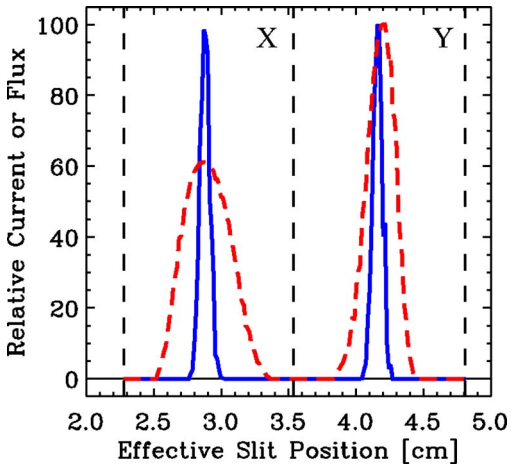

FIG. 4. (Color online) Typical photon (solid curve) and ion (broken curve) beam profiles monitored by the central slit scanner. The two cuts, obtained in perpendicular directions, are used to obtain an estimate of the beam overlap quality.

$$\sigma = \frac{qv}{I\Phi F}R, \tag{2}$$

where the form factor F is a measure of the quality of the overlap of the ion beam with the photon beam.

In the present experiments, profiles of the photon beam and ion beam were obtained in two orthogonal slice directions and at three positions: near the entrance and exit of the interaction region with NEC beam profile monitors, and at the center of the interaction region with a slit scanner. At each of these positions, a two-dimensional (2D) form factor F_z was estimated based on ion (i) and photon (ϕ) beam profiles: $F_z = \int i_x \phi_x dx \int i_y \phi_y dy$, where x and y are orthogonal directions in the plane normal to the ion and photon beam propagation direction. (A typical profile measurement taken on the central slit scanner is shown in Fig. 4.) The total form factor F is obtained by integration of the quadratic interpolation of the three 2D form factors over the interaction region length. In order to estimate the error produced by the interpolation, the form factor is also determined assuming the overlap of the beam does not vary over the interaction region, and is equal to that observed in the center of the interaction region. A difference of less than 1.5% was observed between the two determinations.

The signal rate is given by $R = R_o/\Omega_{\rm det}\Omega_{\rm elect}$, where R_o is the observed count rate, and $\Omega_{\rm det}$ and $\Omega_{\rm elect}$ are the detector and electronics pulse efficiencies, respectively. The efficiencies for He^+ detection in the present experiment were measured to be $\Omega_{\rm det}=0.508(43)$ and $\Omega_{\rm elect}=0.73(1)$.

The main instrumental uncertainties in the cross-section measurements arise from the flux determination (±8.8%), the photoion signal (He^+) collection and detection efficiency (+9.2%/−8.7%), the primary ion beam (He^-) collection and detection efficiency (+0.5%/−2.0%), the form factor measurement and integration (+8.5%/−3.7%), and the ion velocity determination (±0.9%). All errors are assumed to be independent and added in quadrature. A total instrumental

error of +15%/−13% is thus obtained, of which an estimated ±2.8% is due to random effects (e.g., from meter measurements, beam profile monitor instabilities, etc.). An additional uncertainty of ±1.3% to 2.6% is obtained from the ion signal counting statistics. The measurements were repeated several times and two sets of measurements at 38.823 eV were collected in order to verify that all random and long-term drift effects had been accounted for. No significant trends were observed within or between the sets. The absolute cross-section measurement at 38.823 eV is barely in agreement with theory at the 1 SD level, and might suggest a slightly larger cross section than calculations.

In summary, the near-threshold relative and absolute photodetachment cross section has been measured and compared to theory. Photoelectron recapture due to PCI effects has been estimated within the semiclassical approximation and agrees well with observation. Photoelectron recapture is most significant nearer to the threshold and would be observed as a large feature in neutral He production. Direct measurement of this feature would be of obvious interest. We note, however, that the short autodetachment lifetime of He^- [14] would produce a He background on the order of 1 GHz, making detection of the feature exceedingly challenging. Other stable negative ions with strong PCI recapture, such as Li^- [1,22], could make far better potential targets for such an experiment.

We thank B. S. Rude for technical assistance during the experiment and C. W. Walter for helpful comments during the preparation of this manuscript. This work was supported by the Department of Energy, Office of Science–Office of Basic Energy Sciences, Chemical, Geoscience and Biological Divisions. The ALS is funded by the Department of Energy, Scientific User Facilities Division.

[1] H. Kjeldsen, P. Andersen, F. Folkmann, B. Kristensen, and T. Andersen, J. Phys. B **34**, L353 (2001); N. Berrah, J. D. Bozek, A. A. Wills, G. Turri, H.-L. Zhou, S. T. Manson, G. Akerman, B. Rude, N. D. Gibson, C. W. Walter, L. VoKy, A. Hibbert, and S. M. Ferguson, Phys. Rev. Lett. **87**, 253002 (2001).

[2] A. M. Covington, A. Aguilar, V. T. Davis, I. Alvarez, H. C. Bryant, C. Cisneros, M. Halka, D. Hanstorp, G. Hinojosa, A. S. Schlachter, J. S. Thompson, and D. J. Pegg, J. Phys. B **34**, L735 (2001).

[3] D. S. Kim, H. L. Zhou, and S. T. Manson, J. Phys. B **30**, L1 (1997); Phys. Rev. A **55**, 414 (1997).

[4] J. Xi and C. F. Fischer, Phys. Rev. A **59**, 307 (1999).

[5] H. L. Zhou, S. T. Manson, L. Vo Ky, A. Hibbert, and N. Feautrier, Phys. Rev. A **64**, 012714 (2001).

[6] J. L. Sanz-Vicario and E. Lindroth, Phys. Rev. A **65**, 060703(R) (2002); N. Brandefelt and E. Lindroth, *ibid.* **65**, 032503 (2002).

[7] J. L. Sanz-Vicario, E. Lindroth, and N. Brandefelt, Phys. Rev. A **66**, 052713 (2002).

[8] O. Zatsarinny, T. W. Gorczyca, and C. Froese Fischer, J. Phys. B **35**, 4161 (2002).

[9] N. Berrah, J. D. Bozek, G. Turri, G. Akerman, B. Rude, H.-L. Zhou, and S. T. Manson, Phys. Rev. Lett. **88**, 093001 (2002).

[10] R. C. Bilodeau, J. D. Bozek, A. Aguilar, G. D. Ackerman, G. Turri, and N. Berrah, Phys. Rev. Lett. **93**, 193001 (2004).

[11] R. C. Bilodeau, J. D. Bozek, N. D. Gibson, C. W. Walter, G. D. Ackerman, I. Dumitriu, and N. Berrah, Phys. Rev. Lett. **95**, 083001 (2005).

[12] A. M. Covington *et al.*, Phys. Rev. A **66**, 062710 (2002).

[13] J. A. Billen, IEEE Trans. Nucl. Sci. **28**, 1535 (1981).

[14] U. V. Pedersen, M. Hyde, S. P. Møller, and T. Andersen, Phys. Rev. A **64**, 012503 (2001), and references therein.

[15] K. Schulz, M. Domke, R. Püttner, A. Gutiérrez, G. Kaindl, G. Miecznik, and C. H. Greene, Phys. Rev. A **54**, 3095 (1996); R. P. Madden, D. L. Ederer, and K. Codling, Phys. Rev. **177**, 136 (1969).

[16] E. Lindroth, Phys. Rev. A **49**, 4473 (1994), and references therein.

[17] A. Niehaus, J. Phys. B **10**, 1845 (1977); G. B. Armen and J. C. Levin, Phys. Rev. A **56**, 3734 (1997).

[18] G. W. F. Drake, Nucl. Instrum. Methods Phys. Res. B **31**, 7 (1988).

[19] Using 1 a.u. = 27.211 384 5(23)μ_m eV = 27.207 655 0 eV, where μ_m is the ^{4}He nucleus-electron reduced mass. P. J. Mohr and B. N. Taylor, Rev. Mod. Phys. **72**, 351 (2000).

[20] Yu. Ralchenko *et al.*, NIST Atomic Spectra Database (version 3.0.1). Online: http://physics.nist.gov/asd3 [2005, March 16].

[21] P. Kristensen, U. V. Pedersen, V. V. Petrunin, T. Andersen, and K. T. Chung, Phys. Rev. A **55**, 978 (1997).

[22] T. W. Gorczyca, O. Zatsarinny, H.-L. Zhou, S. T. Manson, Z. Felfli, and A. Z. Msezane, Phys. Rev. A **68**, 050703(R) (2003).